



## Negative porosity issue in the Heckel analysis: A possible solution

Devang Patel<sup>1</sup>, Vivek D. Patel<sup>1</sup>, Robert Sedlock, Rahul V. Haware<sup>\*</sup>

Natoli Scientific-A Division of Natoli Engineering Company, Inc., Telford, PA 18969, USA

### ARTICLE INFO

#### Keywords:

Heckel analysis  
Modified Heckel equation  
Negative porosity  
Pycnometric tablet density  
Pycnometric powder density  
Relative density  
True density

### ABSTRACT

A parameterization of compaction simulator generated dynamic compression profile with a few grams of powder provides important information about the material deformation and compact elasticity. The Heckel equation is by far the most popular choice among pharmaceutical scientists for such parametrization. A general approach of Heckel analysis uses pycnometric powder density ( $\rho_{p0}$ ) for relative density calculation. However, as 'in-die' tablet bulk density at applied compression pressure ( $\rho_{BP}$ ) becomes greater than or equal to the measured  $\rho_{p0}$ , the general approach typically poses a negative porosity challenge at high compression pressure regions. It is only theoretically possible to have a tablet with zero or negative porosity. Negative porosity may be detected during 'in-die' compression analysis, but it will not exist after ejection of the tablet in practical aspect. Thus, the present work proposes a new approach to using pycnometric tablet density ( $\rho_{pp}$ ) in the relative density calculations of Heckel analysis. This  $\rho_{pp}$  may be a better representation of actual tablet particle volume, as it is composed of non-accessible intra-particulate pores, which are broken under applied compression pressure. A new approach showed its immunity for Heckel high-pressure negative porosity. It enables the utilization of the compression and decompression phases of dynamic compression profiles to evaluate macroscopic compaction performance. The proposed approach was validated with a reported modified Heckel approach. The Heckel parameters computed with both methodologies for microcrystalline cellulose and lactose were not statistically different. However, a modified Heckel approach was unable to compute Heckel parameters of poorly compacting starch unlike the new approach. A modified Heckel approach became invalid during starch compaction at low compression pressures (below 400 MPa), where starch was forming weaker but still intact tablets. Certainly, a complete Heckel profiling with a new approach could save time and costs in an early development stage for designing and screening scientifically based lead prototype formulations.

### 1. Introduction

A powder densification in the pharmaceutical compaction process is a response of bulk powder to the applied compression pressure. This simple-looking biphasic transformation results from several interdependent sequential processes. A bulk powder goes through a series of pressure-dependent events before its final densification. These events start with a low-pressure particle rearrangement followed by a particle deformation in the mid-pressure region of the compression phase. The particles' rearrangements and deformation events set the stage for the inter-particulate bonding required for particle densification (Çelik, 2011). The bulk powder experiences its highest densified form in the maximum pressure region of the compression phase. A highly densified form then enters the pressure unloading 'decompression phase'. This phase gives stress-relieving opportunity to the highly densified compact.

The densified compact shows a low or high 'in-die' relaxation during the unloading of the compression phase, depending on its composition (Govedarica et al., 2012; Haware et al., 2010b). Thus, a transformation of powder bulk into a densified form is a multi-step complex process. It is critical to understand the relationship between consolidation pressure and material properties to optimize the formulation design and tablet manufacturing process (He et al., 2018). The mathematical modeling of such a complex process with a simple formula is highly unrealistic. Several compression equations like Heckel, Walker, Kawakita, and Shapiro are used alone and/or in combinations to provide explanatory predictive response of material during the compression process (Heckel, 1961a; Kawakita, 1963; Shapiro and Kolthoff, 1947; Walker, 1923). Out of these equations, the Heckel equation has by far been the most popular among pharmaceutical scientists.

R. W. Heckel, a metallurgist, used this equation in 1961 to understand the compaction behavior of iron, copper, nickel, and tungsten

<sup>\*</sup> Corresponding author at: 100 Emlen Way, Suite #108, Telford, PA 18969, USA.

E-mail address: [rhaware@natoli.com](mailto:rhaware@natoli.com) (R.V. Haware).

<sup>1</sup> Authors have contributed equally.

**List of abbreviations****Abbreviations Definitions**

$V_{PO}$	It is defined as the pycnometric particle volume
$\rho_{PO}$	It is defined as the pycnometric particle density
$m$	It is defined as the mass of the tablet
$\rho_{PP}$	It is defined as the pycnometric tablet density. It is measured by using tablet during Helium pycnometric test
$V_{BO}$	It is defined as the volume of powder between the punch tips without applying any compression pressure or 'in-die' powder bulk volume at zero compression pressure
$\rho_{BO}$	It is defined as the 'in-die' powder bulk density at zero compression pressure. ( $\rho_{BO} = \frac{m}{V_{BO}}$ )
$V_{BP}$	It is defined as the volume of tablet between the punch tips during compression or 'in-die' tablet bulk volume at applied compression pressure
$\rho_{BP}$	It is defined as the 'in-die' tablet bulk density at applied compression pressure. ( $\rho_{BP} = \frac{m}{V_{BP}}$ )
$\rho_{tablet}$	It is defined as 'out of die' tablet bulk density
$\rho_{particle}$	It is defined as particle density calculated from modified Heckel equation
<b>Porosity<sub>0</sub></b>	It is defined as 'In-die' powder porosity at zero compression pressure obtained from force-displacement data. ( $Porosity_0 = 1 - \frac{m/V_{BO}}{\rho_{PO}}$ ) (General Approach). ( $Porosity_0 = 1 - \frac{m/V_{BO}}{\rho_{PP}}$ ) (New Approach)
<b>Porosity<sub>P</sub></b>	It is defined as 'In-die' tablet porosity at applied compression pressure obtained from force-displacement data. ( $Porosity_P = 1 - \frac{m/V_{BP}}{\rho_{PO}}$ ) (General Approach) ( $Porosity_P = 1 - \frac{m/V_{BP}}{\rho_{PP}}$ ) (New Approach)

(Heckel, 1961a, 1961b). The compaction behavior of these materials was tested in the pressure range of 10,000 psi (~6.89 MPa) to 120,000 psi (827.37 MPa). This pressure range is much too high for typical pharmaceutical materials, as they are either predominantly plastic, elastic, or fragmenting. Heckel considered powder compaction is like the first order chemical kinetics. The powder pores are considered reactants under applied pressure, and powder densification is the final product. The "kinetics" of the compaction process is described as the change in the powder density with pressure and pore fractions.

$$\frac{dD}{dP} \propto (1-D) \quad (1)$$

$$1-D = \text{Pore fractions at pressure } P \quad (2a)$$

$$1-D_0 = \text{Pore fractions at zero pressure} \quad (2b)$$

where,  $D$  is the 'at-pressure' relative density,  $P$  is the compression pressure, and  $D_0$  is the zero-pressure relative density.

$$\frac{dD}{dP} = k(1-D) \quad (3)$$

$$\frac{dD}{(1-D)} = kdP \quad (4)$$

$$\int_{D_0}^D \frac{dD}{(1-D)} = k \int_0^P dP \quad (5)$$

$$\ln D - \ln(1-D) = kP \quad (6)$$

$$\ln(1-D_0) - \ln(1-D) = kP \quad (7)$$

$$-\ln(1-D) = kP - \ln(1-D_0) \quad (8)$$

$$\ln \frac{1}{(1-D)} = kP + \ln \frac{1}{(1-D_0)} \quad (9)$$

$$\ln \frac{1}{(1-D)} = kP + A \quad (10)$$

$$\text{where, } A = \ln \frac{1}{(1-D_0)}$$

Eq. (10) is a widely accepted form of the Heckel equation in the pharmaceutical sciences. The relative density is a ratio of 'in-die' tablet bulk density at applied compression pressure ( $\rho_{BP}$ ) of the material to the pycnometric particle density ( $\rho_{PO}$ ).

$$D = \frac{\rho_{BP}}{\rho_{PO}} \quad (11)$$

$$(1-D) = \left(1 - \frac{m/V_{BP}}{m/V_{PO}}\right) \quad (12)$$

$$(1-D) = \left(\frac{V_{BP} - V_{PO}}{V_{BP}}\right) \quad (13)$$

where,  $V_{BP}$  and  $V_{PO}$  represent 'in-die' tablet bulk volume at applied compression pressure and pycnometric particle volume respectively. We can get the following final Heckel formula (Equation (14)) after substituting Equation (13) into Equation (10).

$$\ln \frac{V_{BP}}{V_{BP} - V_{PO}} = kP + A \quad (14)$$

**1.1. Three possible scenarios of the Heckel equation**

As mentioned earlier, the Heckel equation was initially developed to test the compression behavior of metal powders. It is also important to note that Heckel has used only the compression phase to evaluate materials in his first paper. The Young's moduli of tested metals ranges between copper (117 GPa) and tungsten (400–410 GPa). These materials are less elastically deformable than typical pharmaceutical powders. The Young's moduli of typical pharmaceutical powders are below 20 GPa (Bassam et al., 1990; Roberts and Rowe, 1987). Moreover, the applied compression pressure was in the range of 6.87 MPa to 827.37 MPa (Heckel, 1961a). This is an extremely high compression pressure range, as the pharmaceutical processes are typically operated between ~50 to ~250 MPa compression pressure depending on the formulation composition.

The relative density in the original Heckel publication is defined as "the ratio of the density of the compact to that of the metal without porosity" (Heckel, 1961b). Material density without porosity is called "true density". Pharmaceutical scientists have interpreted "density without porosity or true density" as the "pycnometric particle density" of the material while it is measured using a Helium pycnometer. The accuracy of pycnometric particle density has its own challenges, as Helium cannot intercept its way in the closed intra-particulate voids. Therefore, the measured pycnometric particle density is not a "true density" as it does not exclude intra-particulate void volumes completely. The pycnometric particle density at zero pressure could be different after applying pressure. A simple experiment performed on a spray-dried coffee powder showed a 1.3% difference in zero pressure particle volume and measured after applying hand pressure required to break large particles (data not shown) (Fig. 1). This particle volume difference translates into a difference of 1.04% in the computed particle density values. Additionally, data represented in Table 1 reveals that pycnometric particle density ( $\rho_{PO}$ ) is different than the pycnometric tablet density ( $\rho_{PP}$ ). It is dependent on the applied compression pressure. The  $\rho_{PO}$  is always lower than the  $\rho_{PP}$ . However, the relative density

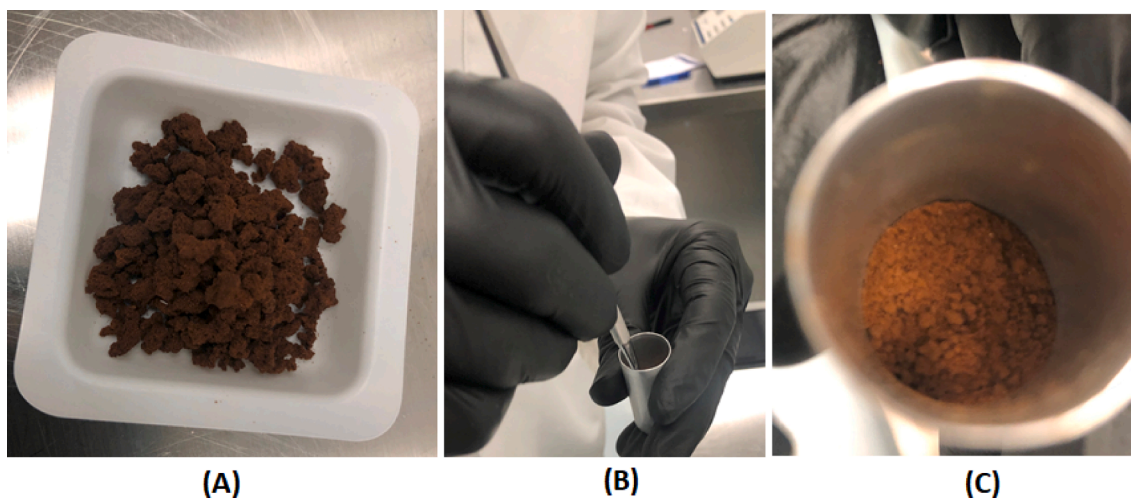


Fig. 1. Change in the particle dimension of spray-dried coffee powder after hand-trituration (A) 'As-is' spray dried coffee powder; (B) Hand trituration of coffee powder; (C) Triturated coffee powder.

calculations of Heckel analysis uses the ratio of  $\rho_{BP}$  of the material to  $\rho_{P0}$ . In the initial stage of the compression cycle, the  $\rho_{P0}$  is always higher than the 'in-die' powder bulk density ( $\rho_{B0}$ ) of the material. This scenario might not be true for  $\rho_{BP}$  calculated in the Heckel analysis with a continuous compression profile generated by a compaction simulator. The pharmaceutical materials undergo fragmentation and deformation under the applied compression load. This could possibly destroy the intra-particulate pores, which might not be measured by Helium pycnometer at  $\rho_{P0}$  analysis. Consequently, the initial measured  $\rho_{P0}$  is possibly lower than the  $\rho_{PP}$ . The change in these particle densities could primarily depend on particle morphology and dimensions, as well as the deformation and fragmentation propensity of the materials (Fichtner et al., 2007; van den Ban and Goodwin, 2017). Therefore,  $\rho_{BP}$  values could eclipse the  $\rho_{P0}$ , specifically at the high compression pressure. The following three possible scenarios between the  $\rho_{BP}$  and  $\rho_{P0}$  could be experienced depending on the applied compression pressure (Fig. 2).

#### 1.1.1. Zone I [ $\rho_{BP} < \rho_{P0}$ ( $V_{BP} > V_{P0}$ )]

The first zone indicates that  $\rho_{BP}$  is always lower than the  $\rho_{P0}$  or  $V_{BP}$  is always greater than  $V_{P0}$  (Fig. 2). This relationship is valid for most of the pharmaceutical compression processes operated at low compression pressure. This is ideal for evaluating the compaction simulator or emulator-generated dynamic compression profile with the Heckel equation. Heckel equation remains valid for both compression and decompression phases in the entire compression pressure range when  $\rho_{BP} < \rho_{P0}$  (or  $V_{BP} > V_{P0}$ ). This allows efficient use of the decompression phase to evaluate tablet 'in-die' elastic recovery. It is useful information for evaluating material deformation and other tableting issues such as capping and lamination.

#### 1.1.2. Zone II [ $\rho_{BP} \approx \rho_{P0}$ ( $V_{BP} \approx V_{P0}$ )]

In the second zone,  $\rho_{BP}$  or  $V_{BP}$  and  $\rho_{P0}$  or  $V_{P0}$  become equal (Fig. 2). When we substitute these values in Equation (14), it becomes undefined (Equation (15)):

$$\ln \frac{V_{BP}}{V_{BP} - V_{BP}} = kP + A \quad \therefore \ln \frac{V_B}{0} = kP + A \quad (15)$$

#### 1.1.3. Zone III [ $\rho_{BP} > \rho_{P0}$ ( $V_{BP} < V_{P0}$ )]

The third zone consists of eclipsing of  $\rho_{BP}$  over  $\rho_{P0}$  (Fig. 2). It demonstrates better densification of the powder at the applied compression pressure. As pressure increases,  $\rho_{BP}$  becomes larger than  $\rho_{P0}$ , which is practically impossible. After application of this scenario to Equation (14), the Heckel equation transforms as follows (Equation (16)):

$$\ln \frac{V_{BP}}{V_{BP} - V_{P0}} = kP + A \quad \therefore -\ln N = kP + A \quad (16)$$

where,  $N$  indicates any real number.

Thus, in the case of the Zones II and III, the Heckel equation becomes invalid, specifically at high compression pressure ranges, where  $\rho_{BP}$  and  $\rho_{P0}$  approaches to equality or  $\rho_{BP}$  becomes larger than  $\rho_{P0}$ . This situation continues in the decompression range. It is termed as a well-known 'negative porosity' issue of Heckel analysis. These scenarios uncover an instance in which it is impossible to parametrize the decompression phase of a continuous compression profile with an 'in-die' Heckel approach. A continuous compression profile is an important tool, especially in the early development stages of formulations, where only a few grams of the pharmaceutical materials are available for the pre-formulation scientist. The extraction of macroscopic deformation material behavior from a continuous compression profile is necessary for developing sound scientifically based lead robust formulation for further development. This can significantly reduce development time and costs.

Additionally, as reported by J. M. Sonnergaard, the logarithmic transformations used in the normalization of  $V_{BP}$  using  $\rho_{P0}$  are extremely sensitive to the possible errors associated with the particle density measurements. Sonnergaard reported that a 1% error in the particle density (1.485 g/cm<sup>3</sup> instead of 1.515 g/cm<sup>3</sup>) could have >10% error in the apparent yield pressure estimates (88 MPa instead of 111 MPa for a true slope of 0.01 and 1.4 intercept) (Sonnergaard, 1999). It suggests the necessity for extreme care while applying the particle density data in the Heckel parametrization.

#### 1.2. Alternative approaches for modification of Heckel equation

Limitations of the Heckel equation have been reported by Fell and Newton (Fell and Newton, 1971) as well as Rue and Rees (Rue and Rees, 1978) even before Sonnergaard (Sonnergaard, 1999). These researchers reported that the sensitivity of the computed Heckel YPpl is dependent on the employed compaction technique.

Kuentz and Leuenberger further reported a modification of Heckel equation to address the pressure susceptibility of the Heckel equation (Kuentz and Leuenberger, 1999). They proposed a new porosity vs pressure relationship in the relationship in their modified Heckel Equation (Equation (17)).

$$P = \frac{1}{C} \left[ \epsilon - \epsilon_c - \epsilon_c \ln \frac{\epsilon}{\epsilon_c} \right] \quad (17)$$

Table 1

Details of particle densities and Heckel parameters measured and estimated with general, new, and modified Heckel approach [ $\rho_{p0}$ : pycnometric particle density ( $\text{g}/\text{cm}^3$ );  $\rho_{pp}$ : pycnometric tablet density ( $\text{g}/\text{cm}^3$ );  $\rho_{particle}$ : particle density ( $\text{g}/\text{cm}^3$ ) computed with modified Heckel approach; 1/C – Constant;  $(1 - \epsilon_C)$  – Constant; YPpl – Yield pressure of plastic deformation (MPa); YPel – Yield pressure of elastic recovery (MPa)].

Material	Target Compression Pressure (MPa)	Actual Compression Pressure (MPa)	$\rho_{p0}$ ( $\text{g}/\text{cm}^3$ )	$\rho_{pp}$ ( $\text{g}/\text{cm}^3$ )	Modified Heckel Equation Parameters			General Approach (with $\rho_{p0}$ )		New Approach (with $\rho_{pp}$ )		Modified Heckel Approach (with $\rho_{particle}$ )		Tablet Mechanical Strength (MPa)
					$\rho_{particle}$ ( $\text{g}/\text{cm}^3$ )	1/C (MPa)	$1 - \epsilon_C$	YPpl (MPa)	YPel (MPa)	YPpl (MPa)	YPel (MPa)	YPpl (MPa)	YPel (MPa)	
MCC	25	22.5 (0.3) <sup>#</sup>	1.57 (0.00)	1.86 (0.02)	33.22* (0.37)	$2.7 \times 10^5$ ( $2.7 \times 10^4$ )	0.01 (0.00)	47 (3)	775 (28)	62 (4)	1117 (42)	1727 (230)	$3.8 \times 10^4$ (853)	0.56 (0.01)
	50	48.8 (1.7)		1.88 (0.02)	21.71* (0.37)	$9.1 \times 10^4$ ( $1.3 \times 10^3$ )	0.02 (0.00)	70 (2)	1091 (71)	101 (2)	1812 (125)	2071 (37)	$4.8 \times 10^4$ (4261)	1.55 (0.05)
	75	73.9 (0.2)		1.90 (0.01)	20.27* (0.24)	$9.6 \times 10^4$ ( $5.2 \times 10^3$ )	0.02 (0.00)	82 (3)	882 (28)	130 (5)	1693 (130)	2772 (89)	$4.6 \times 10^4$ ( $1.4 \times 10^4$ )	2.56 (0.01)
	100	102.6 (1.3)		1.94 (0.02)	1.95 (0.03)	415 (30)	0.18 (0.00)	88 (0)	792 (17)	153 (4)	1904 (85)	154 (6)	1924 (95)	5.08 (0.09)
	150	148.5 (0.3)		1.85 (0.01)	1.81 (0.01)	346 (5)	0.19 (0.00)	98 (1)	936 (133)	168 (5)	2412 (309)	159 (5)	2267 (348)	7.23 (0.23)
	200	200.2 (1.9)		1.68 (0.01)	1.65 (0.01)	237 (5)	0.19 (0.00)	103 (2)	530 (41)	137 (1)	1040 (71)	133 (3)	941 (64)	9.20 (0.12)
	500	502.6 (2.2)		1.68 (0.02)	1.65 (0.01)	279 (10)	0.23 (0.04)	112 (2)	**	193 (10)	813 (42)	171 (9)	632 (58)	***
	550	552.4 (2.5)		1.66 (0.02)	1.64 (0.01)	319 (17)	0.29 (0.01)	116 (3)	**	216 (17)	542 (70)	186 (10)	586 (29)	***
Starch	25	24.7 (0.3)	1.50 (0.00)	**	62.52* (2.10)	$2.4 \times 10^6$ ( $5.3 \times 10^4$ )	0.01 (0.00)	69 (2)	477 (39)	**	**	8023 (430)	$6.7 \times 10^4$ ( $6.8 \times 10^3$ )	**
	50	49.1 (0.6)		**	65.07* (0.44)	$2.5 \times 10^6$ ( $7.5 \times 10^4$ )	0.01 (0.00)	79 (3)	415 (38)	**	**	$1.1 \times 10^4$ (306)	$8.0 \times 10^4$ ( $6.7 \times 10^3$ )	**
	75	73.6 (0.3)		**	65.24* (0.48)	$2.5 \times 10^6$ ( $2.7 \times 10^4$ )	0.01 (0.00)	90 (1)	725 (50)	**	**	$1.4 \times 10^4$ (272)	$1.9 \times 10^5$ ( $2.5 \times 10^4$ )	**
	100	97.8 (2.8)		1.74 (0.02)	63.92* (10.19)	$2.8 \times 10^6$ ( $8.9 \times 10^6$ )	0.01 (0.00)	115 (2)	846 (30)	180 (8)	1670 (119)	$1.7 \times 10^6$ ( $3.3 \times 10^6$ )	$2.2 \times 10^6$ ( $3.9 \times 10^6$ )	0.37 (0.03)
	150	146.0 (0.8)		1.71 (0.01)	64.44* (6.46)	$3.2 \times 10^6$ ( $7.5 \times 10^6$ )	0.01 (0.00)	121 (1)	617 (58)	191 (4)	1437 (146)	$2.2 \times 10^6$ ( $2.5 \times 10^6$ )	$2.5 \times 10^6$ ( $4.1 \times 10^6$ )	0.71 (0.01)
	200	195.9 (4.6)		1.74 (0.03)	2.92* (0.41)	4212 (1455)	0.25 (0.03)	112 (5)	361 (43)	208 (6)	1317 (31)	686 (147)	6135 (1379)	1.10 (0.06)
	400	402.6 (3.9)		1.70 (0.02)	1.62 (0.00)	400 (23)	0.35 (0.01)	95 (3)	**	245 (11)	1253 (82)	173 (5)	713 (70)	1.58 (0.13)
	450	447.4 (1.3)		1.73 (0.02)	1.61 (0.01)	382 (28)	0.35 (0.01)	93 (2)	**	285 (2)	1145 (143)	169 (7)	463 (95)	1.44 (0.17)
Lactose	25	22.5 (2.0)	1.54 (0.01)	1.57 (0.01)	2.57* (0.37)	1644 (599)	0.30 (0.05)	48 (2)	753 (54)	50 (2)	803 (58)	134 (35)	2568 (135)	0.34 (0.03)
	50	45.4 (1.9)		1.57 (0.02)	1.49 (0.04)	295 (15)	0.45 (0.00)	78 (7)	1166 (123)	82 (7)	1253 (104)	170 (2)	1001 (144)	0.35 (0.03)
	75	74.1 (2.6)		1.56 (0.01)	1.53 (0.07)	348 (82)	0.47 (0.04)	109 (2)	1640 (129)	114 (1)	1769 (106)	106 (20)	1383 (145)	0.75 (0.06)
	100	101.1 (2.0)		1.56 (0.00)	1.54 (0.01)	378 (12)	0.45 (0.01)	117 (1)	1046 (89)	121 (1)	1107 (86)	118 (3)	1055 (79)	0.82 (0.06)
	150	145.7 (0.5)		1.56 (0.01)	1.55 (0.03)	569 (76)	0.45 (0.00)	183 (2)	1660 (104)	190 (5)	1753 (60)	189 (13)	1736 (60)	1.19 (0.12)
	200	200.2 (4.3)		1.55 (0.01)	1.54 (0.02)	616 (84)	0.46 (0.01)	205 (1)	1597 (46)	210 (3)	1658 (14)	207 (12)	1613 (181)	1.73 (0.20)
	600	586.6 (3.2)		1.55 (0.01)	1.55 (0.01)	558 (11)	0.45 (0.00)	167 (8)	**	179 (5)	401 (68)	186 (12)	445 (123)	5.86 (0.58)
	650	646.3 (1.3)		1.55 (0.00)	1.56 (0.02)	636 (45)	0.44 (0.02)	173 (7)	**	190 (4)	275 (4)	192 (26)	356 (146)	6.45 (0.04)

<sup>#</sup> Value in parenthesis indicates standard deviation; (n = 3).

\* These unrealistically high values of particle densities confirm the inability of modified Heckel approach to remain invalid at low compression pressure regardless of forming intact compact.

\*\* Indicates the inability of the 'general approach' to compute YPel due to negative porosity.

\*\*\* Indicates the inability of the hardness tester to measure breaking force of the tablet. Tablets are too strong at these applied compression pressure and impossible to break on the hardness tester.

### Indicates that data is not available. Tablets produced at applied compression condition are very weak which makes it impossible to collect further data.

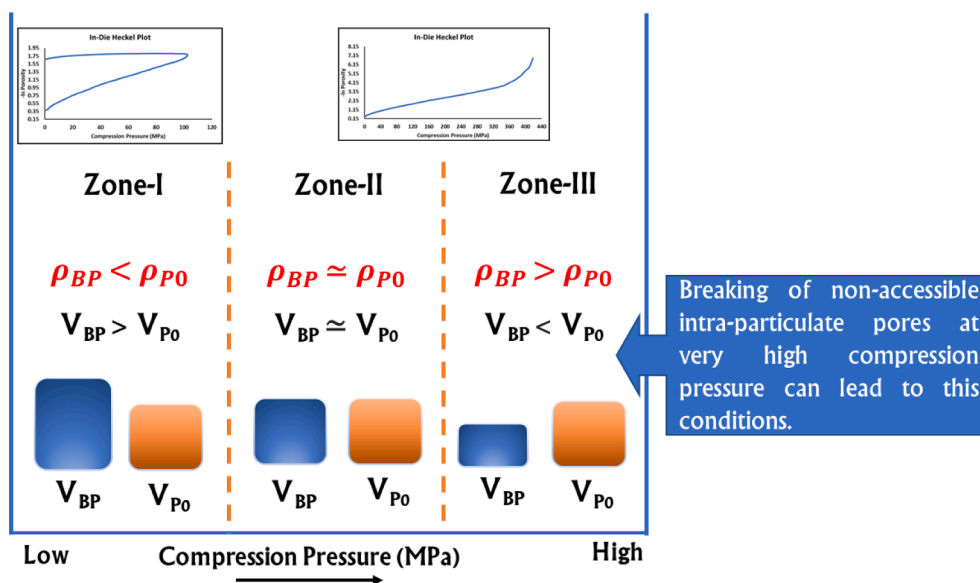


Fig. 2. Possible scenarios between ‘in-die’ tablet bulk density ( $\rho_{BP}$ ) and pycnometric particle density ( $\rho_{P0}$ ) when compression pressure is applied.

where  $P$  is the compaction pressure (MPa),  $C$  is the constant indicating material deformation at  $P$ ,  $\epsilon$  is the porosity, and  $\epsilon_C$  is the critical porosity. They analyzed differently deforming materials using tablet’s ‘out-of-die’ measurements. Interestingly, the calculated  $C$  parameter from a modified Heckel equation for different grades and brands of microcrystalline celluloses such as Emcocel 50 M, Avicel® PH 101, and Avicel® PH 102 were 0.006, 0.007, and 0.008, respectively (Kuentz and Leuenberger, 1999). Clearly, the modified methodology was unable to distinguish material deformability of similarly deforming materials. This was not the case in our previous investigation with ‘in-die’ Heckel analysis of these materials (Haware et al., 2010a). It is also important to note that none of these authors parameterized the decompression phase to compute YPel. Paronen (Paronen, 1986) first reported compact elastic recovery (YPel) from a continuous compression profile using the Heckel approach.

Kuentz and Leuenberger’s modified Heckel approach was further revised by Sun (Sun, 2004) to compute the true density from tablet density versus pressure data (Equation (18)).

$$P = \frac{1}{C} \left[ \left( 1 - \epsilon_C \right) - \frac{\rho_{\text{tablet}}}{\rho_{\text{true}}} - \epsilon_C \ln \left( \frac{1 - \frac{\rho_{\text{tablet}}}{\rho_{\text{true}}}}{\epsilon_C} \right) \right] \quad (18)$$

where,  $\rho_{\text{tablet}}$  is the ‘out of die’ tablet bulk density, and  $\rho_{\text{true}}$  is the particle density. This method involves nonlinear regression of compaction-pressure tablet density data to compute three constants  $C$ ,  $\epsilon_C$ , and  $\rho_{\text{true}}$ . As mentioned earlier, it is not possible to get true density of the materials. Therefore,  $\rho_{\text{particle}}$  will be used instead of  $\rho_{\text{true}}$  in the present report.  $\rho_{\text{particle}}$  is defined as particle density calculated from modified Heckel equation. Author demonstrated good reliable predictions of particle densities for materials forming intact tablets from the compaction data. However, this approach was unable to compute particle densities of materials, which do not form the intact tablets (Sun, 2004).

There are several mathematical models available with modification of Heckel equation, which are mostly empirical or contain at least some experimental components (Cartensen et al., 1990; Denny, 2002; Yu and Hall, 1994). Thus, the hypothesis of the present work was that applying  $\rho_{pp}$  of material in the relative density calculations of Heckel analysis could overcome the negative porosity issues associated with the high compression pressure ranges of the continuous compression profiles. The proposed methodology was also validated by comparing calculated Heckel parameters with our new approach to that of calculated with  $\rho_{\text{particle}}$  using Kuentz, Leuenberger, and Sun’s combined modified Heckel

approach (Kuentz and Leuenberger, 1999; Sun, 2004).

The hypothesis was tested by using predominantly plastic [Microcrystalline cellulose (Vivapur® 101)], elastic [Pregelatinized starch (Starch 1500®)], and fragmenting material [ $\alpha$ -lactose monohydrate (Tabletose® 100)].

## 2. Materials

Microcrystalline cellulose (Vivapur® 101, Lot no. V101C20G62, JRS Pharma LP, NY), partially pregelatinized maize starch (Starch 1500®, Lot no. IN544252, Colorcon Inc, PA), and  $\alpha$ -lactose monohydrate (Tabletose® 100, Lot no. L104294020, Meggle Pharma, Germany) were used as model materials in this study. All materials were used as received.

## 3. Methods

### 3.1. Particle density

All powder materials were used ‘as-is’ for pycnometric analysis and subsequent tableting. The pycnometric particle density of each material was measured using helium displacement pycnometer (AccuPyc™ II 1340, Micromeritics GmbH, Neuss, Germany). Enough powder samples were weighed using an analytical balance (Model EBL 164e, Adam Equipment, Oxford, CT) that filled about  $\frac{3}{4}$ th volume of the sample cell. The experiment was ended when the variation among five consecutive measurements was less than 0.005%. The mean of the last five measurements was taken as the sample pycnometric particle density ( $\rho_{P0}$ ).

The tablets made from ‘as-is’ powder materials were used for pycnometric density analysis. The weight of tablets prepared at different pressures was measured on an analytical balance. The tablet was placed in the sample cell of the helium displacement pycnometer. Then five repetitive cycles for each sample were performed, and the mean of these five measurements was recorded as the pycnometric tablet density ( $\rho_{PP}$ ).

The particle size distribution of MCC, starch, and lactose were taken from previous literatures.  $D_{20}$ ,  $D_{50}$ , and  $D_{90}$  values for MCC are reported as 4, 38, and 70, respectively (Haware et al., 2010a).  $D_{50}$  and  $D_{90}$  values of starch are reported as 140 and 171, respectively (Haware et al., 2009a).  $D_{10}$ ,  $D_{50}$ , and  $D_{75}$  values of lactose are reported as 73, 149, and 220, respectively (Haware et al., 2009b).

### 3.2. Dynamic compression profiling

Continuous dynamic compression profiles of MCC, starch, and lactose powder were generated using the compaction emulator (Presster™, Natoli Scientific, PA) under different compression conditions. A 28 station Natoli NP-400 tablet rotary press (Natoli Engineering, St Charles, MO) profile was emulated on the Presster to compress tablets. Presster™ was calibrated by the Original Equipment Manufacturer (OEM) using National Institute of Standards and Technology (NIST) traceable standards certified through an ISO 17025 accredited laboratory. The calibration factors for all strain gauges (full Wheatstone bridge) and linearly variable differential transformers (LVDTs) were determined by linear regression of calibration data with  $R^2 > 0.999$ . The obtained force–displacement data is not corrected for the punch-to-punch deformation, as such dynamic calibration of Presster is not possible with the current set-up of Presster. Presster was armed with a 250 mm diameter compaction roll and round flat-faced “B” 10 mm tooling for this study. Each powder material was compressed at 25, 50, 75, 100, 150, and 200 MPa with a linear velocity of 0.35 m/sec. Additionally, MCC was compressed at 500 and 550 MPa, starch was compressed at 400 and 450 MPa, and lactose was compressed at 600 and 650 MPa with a linear velocity of 0.35 m/sec to achieve a possible ‘in-die’ Heckel negative porosity. Tablet fill weight was determined using a theoretical constant particle volume of  $0.1913 \pm 0.0005 \text{ cm}^3$ . The reason for using the constant particle volume was due to the response to punch movement being a function of the volume of solid in a die rather than its mass (Çelik and Okutgen, 1993). The powder was weighed and fed manually into the die and then compressed at the above-mentioned compression parameters. The punches and die were externally lubricated with 1.0 %w/v magnesium stearate-acetone suspension before each compression. Tablet weight was determined immediately after the tablet ejection from the die. Breaking force of the tablets were measured (PharmaTest PTB 511E, ISO 9001, Hainburg, Germany) and tablet mechanical strength (TMS) were calculated using following Equation (19) (Newton et al., 1971).

$$TMS = \frac{2F}{\pi Dt} \quad (19)$$

where,  $F$  is the breaking force (N),  $D$  is diameter (mm), and  $t$  is the thickness of tablet (mm).

### 3.3. Heckel parametrization of ‘in-die’ compression profiles

The obtained compression profile was parameterized with the Heckel equation (Equation (10)).

#### 3.3.1. Relative density with a general approach

A relative density component of the Heckel equation is generally computed as a ratio of  $\rho_{BP}$  to  $\rho_{P0}$ . Heckel uses a logarithmic density normalization. Such logarithmic transformations are extremely sensitive to small errors in the powder weight measurement. A small variation in the powder weight could significantly impact the final yield pressure values. The manual material transfer in the die is not immune to unavoidable powder weight loss. Therefore, the tablet weight after ejection from the die, instead of the initial pre-compression material powder weight, was used for calculating  $\rho_{BP}$ . Moreover, the final tablet weight correctly represents the solid fraction contributing to the tablet formation. This is our routine laboratory procedure for the Heckel parametrization of dynamic compression profiling.

#### 3.3.2. Relative density with a new approach

As we are using post-compression material mass (compact mass) in the Heckel relative density parameterization, it was interesting to see the impact of ‘post-compression’ pycnometric tablet density ( $\rho_{PP}$ ) on the relative density and subsequent yield pressure values calculations.

Therefore, a new approach consisting of a ratio of  $\rho_{BP}$  to  $\rho_{PP}$  was used in the relative density calculations.

#### 3.3.3. Relative density with a modified Heckel approach:

Kuentz, Leuenberger, and Sun’s combined modified Heckel approach was used to compute  $\rho_{particle}$  using Equation (18) (Kuentz and Leuenberger, 1999; Sun, 2004). Kuentz, Leuenberger, and Sun have used ‘out of die’ tablet bulk density ( $\rho_{tablet}$ ) to calculate  $\rho_{particle}$ , while authors have used ‘in-die’ tablet bulk density ( $\rho_{BP}$ ) obtained from force-displacement data. A continuous profile of ‘in-die’ tablet bulk density ( $\rho_{BP}$ ) versus compression pressure was fitted in Equation (18) using a non-linear regression curve fitting function with the Levenberg Marquardt algorithm (Fig. 3) (OriginLab® 2022, OriginLab Corporation, Northampton, MA). The obtained  $\rho_{particle}$  was used to calculate Heckel relative density and subsequent yield pressures.

#### 3.3.4. Heckel yield pressure values

The yield pressure values of plastic deformation (YPpl) and elastic recovery (YPel) was computed in the linear region of compression and decompression phase of a continuous ‘in-die’ Heckel profile. The linear regression analysis was performed in the mid-pressure region of the compression and decompression phase of the Heckel plot. The  $R^2$  value  $> 0.90$  was considered for YP calculations. The reciprocal of the slope values for compression and decompression phases can be defined as YPpl and YPel values, respectively.

#### 3.3.5. Validation of Heckel parameters measured from the new approach with modified Heckel approach

Heckel parameters computed from the new approach with the modified Heckel equation was validated statistically with a one-way ANOVA test. A post-hoc test (Dunnett’s simultaneous test) was used for multiple comparisons with the control group (YPpl and YPel values derived by the new approach) using Prism 9 (GraphPad Software, San Diego, California). The models were deemed to be significant with  $p < 0.05$ .

## 4. Results and discussion

### 4.1. Comparison of $\rho_{P0}$ , $\rho_{PP}$ and $\rho_{particle}$

The  $\rho_{P0}$ ,  $\rho_{PP}$ , and  $\rho_{particle}$  of each material are reported in Table 1. The differences between  $\rho_{PP}$  and  $\rho_{particle}$  of MCC (tablets compressed  $\geq 100$  MPa compression pressure) and lactose (tablets compressed  $\geq 50$  MPa compression pressure) were statistically insignificant ( $0.55 \leq p \leq 0.77$ ). The differences between  $\rho_{PP}$  and  $\rho_{particle}$  of starch compacts formed above 400 MPa compression pressure were statistically significant ( $0.0005 \leq p \leq 0.003$ ). A predicted  $\rho_{particle}$  with a modified Heckel approach for MCC compacts manufactured below 100 MPa compression pressure were  $20.27 \text{ g/cm}^3 - 33.33 \text{ g/cm}^3$ , starch compacts manufactured below 400 MPa compression pressure were  $2.92 \text{ g/cm}^3 - 65.24 \text{ g/cm}^3$ , and lactose compacts manufactured below 50 MPa compression pressure were  $2.57 \text{ g/cm}^3$ . These values are extremely high or unrealistic as compared to measured  $\rho_{P0}$  and  $\rho_{PP}$  of MCC, starch and lactose. MCC and lactose were forming intact tablets throughout the applied compression pressure range, while starch was forming intact tablets above 100 MPa compression pressure range only in the present study. Figure S1 shows that plots of tablets compressed below 100 MPa compression pressure doesn’t coincide with the those compressed above 100 MPa compression pressure. It insinuates a linear pattern of the ‘in-die’  $\rho_{BP}$  versus compression pressure plot at low compression pressures. Such plot followed a nonlinear (exponential) pattern at high compression pressures. Thus, an application of the modified Heckel equation on the tablet compressed at low compression pressure becomes invalid due to modeling of linear pattern with a nonlinear equation. These findings stand true for all studied materials in the present report. It could be the

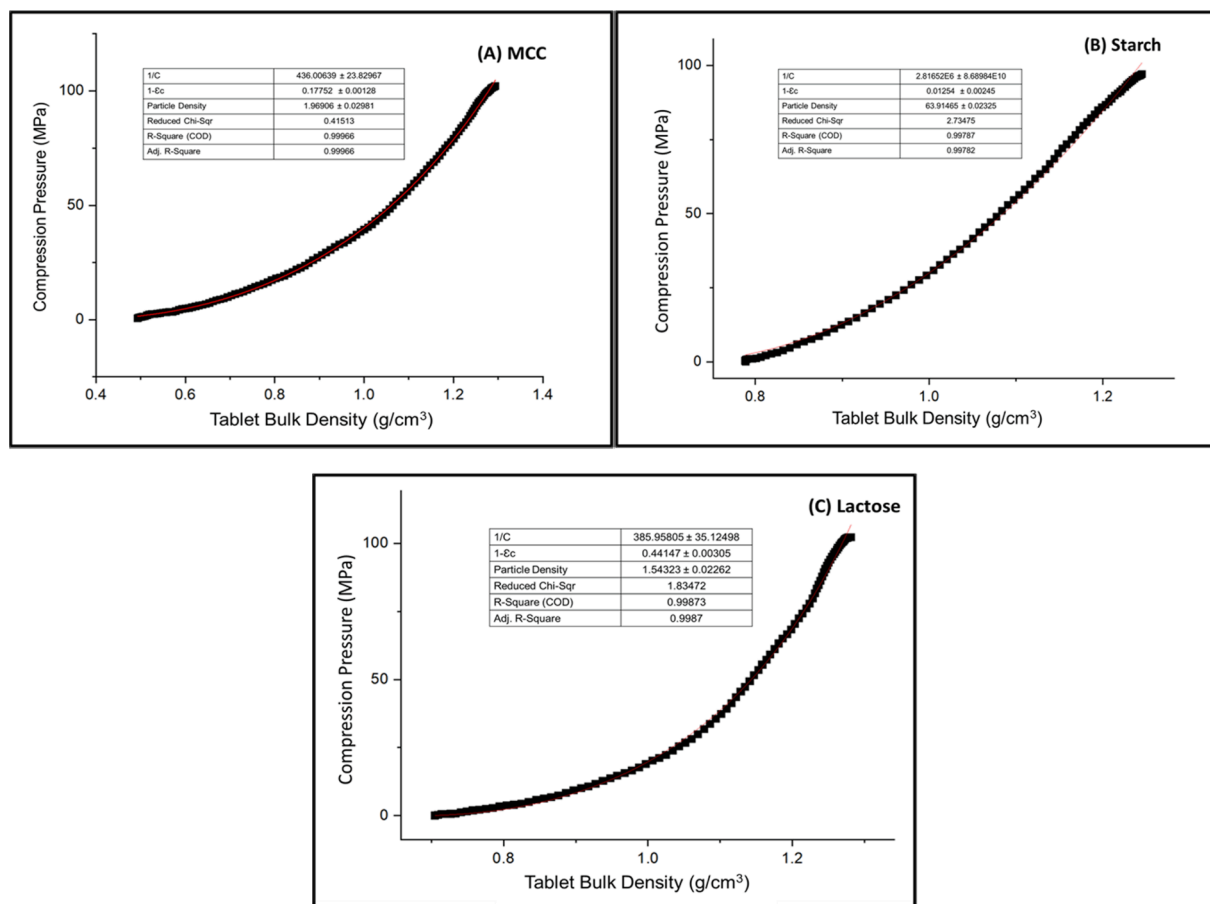


**Fig. 3.** Representative continuous profiles of ‘in-die’ tablet bulk density ( $\rho_{BP}$ ) ( $\text{g}/\text{cm}^3$ ) versus compression pressure (MPa) for (A) MCC, (B) starch, and (C) lactose were fitted in Equation (18) using non-linear regression curve fitting function with Levenberg Marquardt algorithm of OriginLab® 2022 software.

reason for the unrealistically high-density values at low compression pressure with a modified Heckel equation (Table 1). On the other hand, the relationship between ‘in-die’  $\rho_{BP}$  and compression pressure becomes nonlinear with an increment in the compression pressure (Figure S1). A modified Heckel equation becomes valid in this range, which leads to give very close  $\rho_{PP}$  as that of experimental values. The Sun reported that a modified Heckel approach is unable to predict particle densities of materials forming broken tablets (Sun, 2004). Still, the present study demonstrated that the modified Heckel approach is not applicable even for materials forming weaker intact tablets.

The  $\rho_{PP}$  of MCC, starch, and lactose were ~6 to 24%, ~13 to 16%, and ~0.5 to 2% higher than their respective  $\rho_{P0}$ . These differences are more than Sonnergaard’s 1:10 impact ratio of particle density: Heckel apparent yield pressure estimates (Sonnergaard, 1999).

It was interesting to see a decrease in the  $\rho_{PP}$  and  $\rho_{particle}$  for MCC from 102.6 MPa compression pressure. The differences between MCC compact particle densities in the pressure range of 200.2 MPa to 552.4 MPa were not statistically significant ( $p=0.21$ ). MCC tablet formed after 200.2 MPa were extremely strong. Conversely,  $\rho_{PP}$  were less compared to the compact formed at 102.6 MPa. This could be attributed to the applied fill pressure during particle volume analysis. The applied fill pressure, which is a pressure used for helium penetration into the powder or tablet during the pycnometric particle density measurement was 134.4 kPa. This helium pressure may not be sufficient for helium to penetrate the dense compact. The helium pycnometer used in the present experimentation can handle a maximum fill pressure of 3447.4 kPa after being armed with a high-pressure sample chamber (Micromeritics, 2019). The opposite trend of  $\rho_{PP}$  of the stronger tablet could imply the use of a high-pressure helium gas for measuring  $\rho_{PP}$  of denser compacts.

High fill pressure helium density measurements were not carried out in the present study due to the unavailability of a high-pressure sample chamber.

#### 4.2. Heckel parametrization of ‘in-die’ compression profiles

The compression profile obtained at different compression pressures for MCC and lactose were parameterized with a general, new, and modified Heckel approach. A general, new, and modified Heckel approach employs respective  $\rho_{P0}$ ,  $\rho_{PP}$ , and  $\rho_{particle}$  in the relative density calculations. Application of a modified Heckel approach was not possible for MCC tablets manufactured below 100 MPa compression pressure, starch tablets manufactured below 400 MPa compression pressure, and lactose tablets manufactured below 50 MPa compression pressure as this approach was unable to estimate  $\rho_{particle}$  for these tablets accurately. The ‘in-die’ bulk densities ( $\rho_{B0}$ ,  $\rho_{BP}$ ) and porosity ( $Porosity_0$ ,  $Porosity_p$ ) values of the general approach are reported in Table 2. The porosity values,  $Porosity_0$  and  $Porosity_p$  of new approach are also reported in Table 2. Data shows that  $Porosity_p$  computed with general and new approach decreases steadily with increase in ‘In-die’ bulk density ( $\rho_{BP}$ ) at applied compression pressure. This trend was observed for all three model materials.  $\rho_{BP}$  increases with increase in compression pressure and eventually get plateau and exhibits negative porosity issues during Heckel analysis (Table 2).  $Porosity_p$  and relative density computed with general and new approach decreases and increases respectively with increase in compression pressure (Fig. 4A-4C). The same trend was also observed for both,  $Porosity_p$  and relative density, with increase in tablet bulk density ( $\rho_{tablet}$ ) (Fig. 4A’-4C’).

The  $\rho_{PP}$  of MCC tablets compressed at different pressures are given in

**Table 2**  
Primary measurement data for general and new approach.

Material	Target Compression Pressure (MPa)	Actual Compression Pressure (MPa)	$\rho_{PO}$ (g/cm <sup>3</sup> )	$\rho_{PP}$ (g/cm <sup>3</sup> )	'In-die' Bulk Density		'In-die' Porosity				Tablet Bulk Density ( $\rho_{tablet}$ ) (g/cm <sup>3</sup> )
					$\rho_{BO}$ (g/cm <sup>3</sup> )	$\rho_{BP}$ (g/cm <sup>3</sup> )	General Approach		New Approach		
							Porosity <sub>0</sub>	Porosity <sub>p</sub>	Porosity <sub>0</sub>	Porosity <sub>p</sub>	
MCC	25	22.5 (0.3) <sup>#</sup>	1.57 (0.00)	1.86 (0.02)	0.471 (0.002)	0.894 (0.006)	0.700 (0.001)	0.430 (0.004)	0.747 (0.001)	0.519 (0.003)	0.80 (0.00)
	50	48.8 (1.7)		1.88 (0.02)	0.471 (0.010)	1.084 (0.003)	0.699 (0.007)	0.309 (0.002)	0.749 (0.006)	0.423 (0.002)	0.99 (0.01)
	75	73.9 (0.2)		1.90 (0.01)	0.486 (0.003)	1.202 (0.004)	0.690 (0.011)	0.234 (0.003)	0.744 (0.008)	0.368 (0.002)	1.11 (0.00)
	100	102.6 (1.3)		1.94 (0.02)	0.489 (0.001)	1.298 (0.006)	0.689 (0.001)	0.172 (0.004)	0.748 (0.002)	0.331 (0.010)	1.23 (0.01)
	150	148.5 (0.3)		1.85 (0.01)	0.496 (0.001)	1.392 (0.000)	0.684 (0.001)	0.112 (0.000)	0.732 (0.002)	0.247 (0.004)	1.32 (0.00)
	200	200.2 (1.9)		1.68 (0.01)	0.498 (0.000)	1.454 (0.005)	0.682 (0.000)	0.072 (0.003)	0.703 (0.002)	0.132 (0.007)	1.38 (0.00)
	500	502.6 (2.2)		1.68 (0.02)	0.473 (0.007)	1.595 (0.004)	0.698 (0.004)	-0.017 (0.002)	0.718 (0.004)	0.050 (0.007)	1.43 (0.00)
	550	552.4 (2.5)		1.66 (0.02)	0.483 (0.011)	1.594 (0.004)	0.692 (0.007)	-0.017 (0.002)	0.710 (0.004)	0.040 (0.007)	1.44 (0.00)
Starch	25	24.7 (0.3)	1.50 (0.00)	##	0.821 (0.006)	1.062 (0.003)	0.453 (0.004)	0.292 (0.002)	##	##	##
	50	49.1 (0.6)		##	0.818 (0.001)	1.166 (0.003)	0.455 (0.001)	0.224 (0.002)	##	##	##
	75	73.6 (0.3)		##	0.821 (0.007)	1.249 (0.002)	0.453 (0.005)	0.168 (0.001)	##	##	##
	100	97.8 (2.8)		1.74 (0.02)	0.787 (0.002)	1.247 (0.005)	0.476 (0.002)	0.169 (0.004)	0.547 (0.006)	0.282 (0.007)	1.08 (0.00)
	150	146.0 (0.8)		1.71 (0.01)	0.798 (0.017)	1.344 (0.002)	0.468 (0.011)	0.104 (0.001)	0.532 (0.007)	0.212 (0.006)	1.16 (0.00)
	200	195.9 (4.6)		1.74 (0.03)	0.801 (0.004)	1.404 (0.007)	0.466 (0.003)	0.064 (0.005)	0.539 (0.005)	0.191 (0.009)	1.21 (0.00)
	400	402.6 (3.9)		1.70 (0.02)	0.784 (0.001)	1.529 (0.002)	0.478 (0.001)	-0.019 (0.001)	0.545 (0.007)	0.101 (0.013)	1.26 (0.00)
	450	447.4 (1.3)		1.73 (0.02)	0.786 (0.000)	1.544 (0.003)	0.476 (0.000)	-0.029 (0.003)	0.545 (0.005)	0.107 (0.010)	1.26 (0.00)
Lactose	25	22.5 (2.0)	1.54 (0.01)	1.57 (0.01)	0.723 (0.020)	1.105 (0.009)	0.531 (0.007)	0.283 (0.012)	0.539 (0.007)	0.296 (0.012)	1.09 (0.02)
	50	45.4 (1.9)		1.57 (0.02)	0.704 (0.021)	1.145 (0.013)	0.543 (0.003)	0.257 (0.010)	0.551 (0.013)	0.271 (0.010)	1.11 (0.01)
	75	74.1 (2.6)		1.56 (0.01)	0.716 (0.008)	1.234 (0.006)	0.536 (0.012)	0.199 (0.007)	0.541 (0.011)	0.209 (0.009)	1.20 (0.00)
	100	101.1 (2.0)		1.56 (0.00)	0.720 (0.017)	1.285 (0.007)	0.533 (0.011)	0.166 (0.004)	0.537 (0.010)	0.174 (0.004)	1.22 (0.01)
	150	145.7 (0.5)		1.56 (0.01)	0.681 (0.008)	1.294 (0.002)	0.558 (0.005)	0.160 (0.001)	0.562 (0.003)	0.168 (0.005)	1.28 (0.01)
	200	200.2 (4.3)		1.55 (0.01)	0.688 (0.016)	1.332 (0.004)	0.554 (0.011)	0.136 (0.002)	0.556 (0.003)	0.140 (0.004)	1.33 (0.00)
	600	586.6 (3.2)		1.55 (0.01)	0.697 (0.003)	1.538 (0.005)	0.548 (0.002)	0.002 (0.003)	0.550 (0.002)	0.007 (0.002)	1.49 (0.00)
	650	646.3 (1.3)		1.55 (0.00)	0.696 (0.003)	1.546 (0.004)	0.549 (0.002)	-0.003 (0.003)	0.552 (0.003)	0.024 (0.037)	1.49 (0.00)

<sup>#</sup> Value in parenthesis indicates standard deviation; (n = 3).

<sup>##</sup> Indicates that data is not available. Tablets produced at applied compression condition are very weak which makes it impossible to collect further data.

the Fig. 5A. The  $\rho_{PP}$  of MCC tablets produced at compression pressure from 25 MPa to 100 MPa was increasing. These values were decreasing for tablets manufactured between 150 MPa and 550 MPa compression pressure. The  $\rho_{PP}$  of MCC were plateaued between the compression pressure of 200 MPa to 550 MPa. Clearly, MCC is exhibiting three transition points with regards to change in  $\rho_{PP}$ . MCC seems forming moderately strong tablets with a proportional decrease in the porosity with respect to the applied compression pressure in the initial phase of 25 MPa to 100 MPa. This change in porosity seems well measured by Helium pycnometer coupled with a low-pressure chamber. This was not the case for MCC tablets produced above 100 MPa pressure, as it was forming extremely stronger tablets. It might not be possible for low-pressure helium to penetrate inside the stronger MCC tablets produced

at high compression pressure. This could be the reason for decrease in the MCC  $\rho_{PP}$  with increase in the compaction pressure. The MCC compactibility above 200 MPa might have reached to its critical limit, resulting into very limited or no change in the tablet porosity after compressing above 200 MPa. This could be the possible reason for a plateaued  $\rho_{PP}$  of MCC values above 200 MPa compression pressure. A decrease in  $\rho_{PP}$  of lactose was found from 25 MPa to 650 MPa (Fig. 5C). This plot showed three transitions 25 MPa - 50 MPa, 75 MPa - 150 MPa, and 200 MPa - 650 MPa. The  $\rho_{PP}$  of lactose tablets were very close for these three regions, which could be attributed to similar compactibility of lactose tablets in these applied compression pressure regions. Starch was unable to produce tablets with sufficient integrity below 100 MPa. Starch tablets exhibited inconsistent trends unlike MCC and lactose

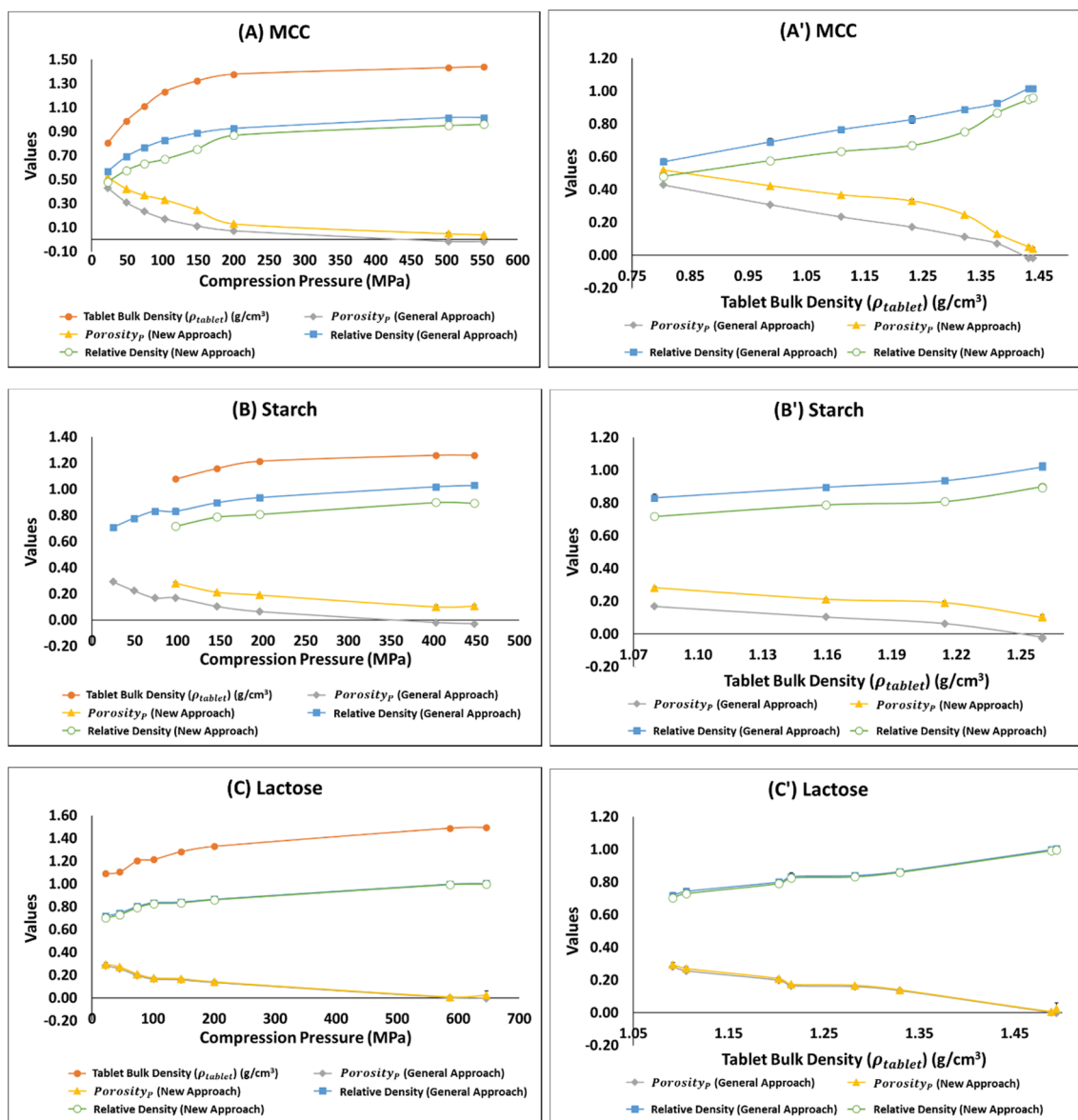


Fig. 4. Plots of pycnometric tablet density ( $\rho_{pp}$ ), tablet bulk density ( $\rho_{tablet}$ ), Porosity<sub>p</sub> and relative density computed with general and new approach vs. compression pressure (MPa) and vs. tablet bulk density ( $\rho_{tablet}$ ).

(Fig. 5B). The change in starch  $\rho_{pp}$  with regards to applied compression pressure is statistically insignificant, which could be attributed to weak tablet formation at applied compression pressures.

Accuracy and repeatability of force-displacement data is crucial for characterizing the material's deformation properties. It was tested by graphing three replicative 'In-die' tablet bulk density (g/cm<sup>3</sup>) vs. compression pressure (MPa) plots of MCC, starch, and lactose at each applied compression pressure (Fig. 6). The superimposed plots of these materials confirmed the ability of Presster™ to produce highly repeatable force-displacement data between multiple runs.

#### 4.2.1. Comparison of general, new, and modified Heckel approach

An 'in-die' Heckel plot of individual MCC tablet with a general, new, and modified Heckel approach is shown in Fig. 7. Heckel analysis at the low-pressure range did not have a negative porosity issue. This could be attributed to the Zone-I scenario (Fig. 2), where the  $\rho_{BP}$  was lower than the  $\rho_{P0}$ . An increment in the compression pressure (>500 MPa) displayed a negative porosity issue (Fig. 7). This could be attributed to the Zone-II or Zone-III scenario (Fig. 2). These zones are characterized with equal or greater  $\rho_{BP}$  than  $\rho_{P0}$ . A high-pressure negative porosity issue

was eliminated with the utilization of  $\rho_{pp}$  and  $\rho_{particle}$  instead of  $\rho_{P0}$  in the Heckel relative density calculations (Fig. 7). A  $\rho_{pp}$  (Table 1) is always higher than  $\rho_{P0}$ . The application of  $\rho_{pp}$  and  $\rho_{particle}$  seems to keep the dynamic Heckel profile in Zone-I and prevents migration to Zone-II and Zone-III. A similar trend was observed with other deforming materials like starch and lactose. Starch and lactose exhibited negative porosity issues >400 MPa, and >600 MPa, respectively. A modified Heckel approach was able to reconcile the negative porosity issue of starch. But this approach could not be applied to starch tablets formed below 400 MPa compression pressure due to its inability to accurately compute  $\rho_{particle}$ , despite forming intact starch tablet (Sun, 2004). This was not the case with our proposed new approach.

#### 4.2.2. Impact of general, new, and modified Heckel approach on YPpl and YPel values

Heckel yield pressure values are well known to be sensitive to various parameters like tooling type, compression pressure, compression speed, blend composition, and compaction simulator type (Rue and Rees, 1978). Heckel yield pressure values would depend on whether the

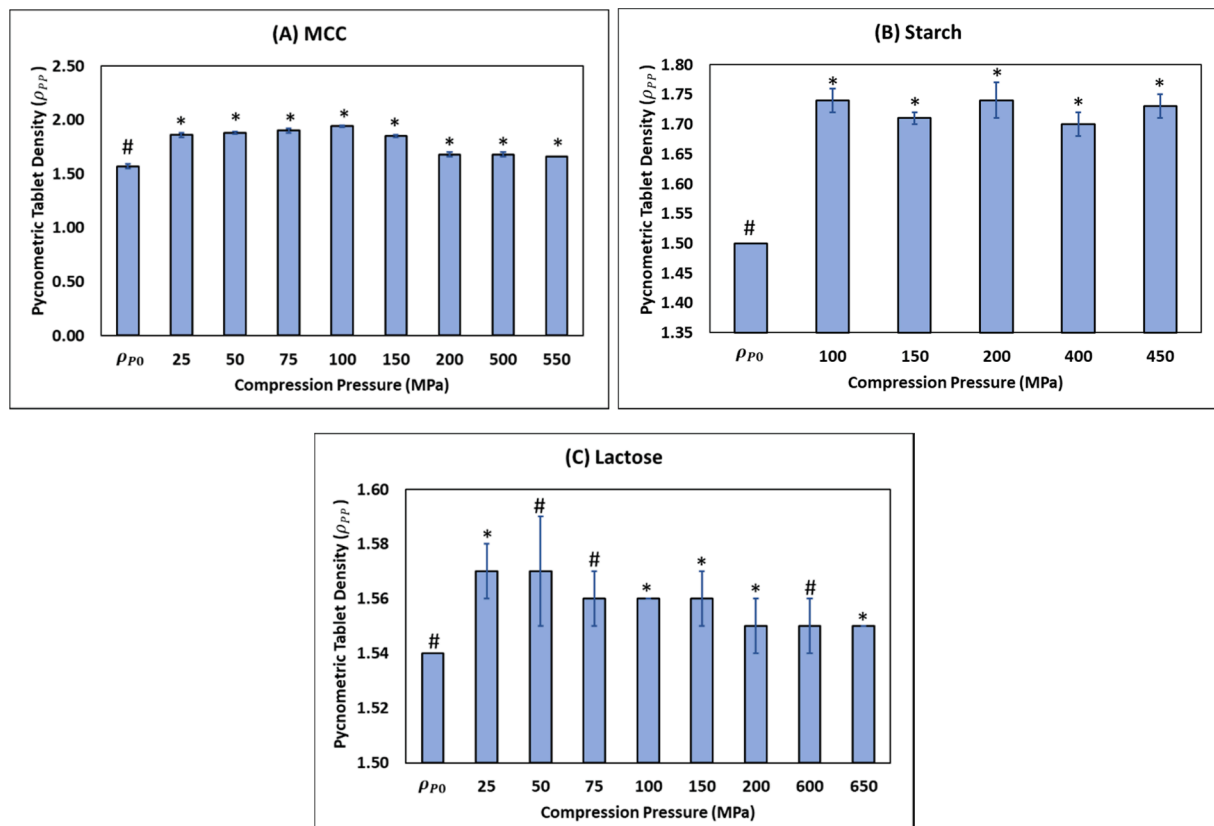


Fig. 5. Plot of pycnometric tablet density ( $\rho_{PP}$ ) vs. compression pressure (MPa) for (A) MCC; (B) Starch; (C) Lactose. Respective pycnometric powder density ( $\rho_{P0}$ ) is also included in each plot. # Indicates there is no statistically significant difference between  $\rho_{PP}$  and  $\rho_{P0}$ . \* Indicates there is statistically significant difference between  $\rho_{PP}$  and  $\rho_{P0}$ .

compaction data are accurately corrected for punch deformation and the compression machine (Çelik, 1992). Due to these reported sensitivities of issues with Heckel parameters, the computed YPpl and YPel with general, new, and modified Heckel approach were compared (Table 1) to evaluate the differences in the computed values by three approaches.

The YPpl values of MCC and lactose tablets (compressed above 100 MPa compression pressure) calculated with a new and modified Heckel approach were 1.29–1.75 and 1.00–1.12 times greater than those calculated with a general approach. The differences between the YPpl values of MCC and lactose calculated with a general approach, and those calculated with a new and modified Heckel approach, were statistically significant ( $0.0001 \leq p \leq 0.0035$ ).

The YPel values of MCC and lactose tablets (compressed above 100 MPa compression pressure) calculated with a new and modified Heckel approach were 1.77–2.43 and 1.02–1.05 times greater than those calculated with a general approach, respectively. The general approach estimated YPel were statistically different ( $0.0001 \leq p \leq 0.0020$ ) from those computed with a new and modified Heckel approach.

It was not possible to compute YPpl and YPel values of MCC tablets manufactured below 100 MPa compression pressure, starch tablets manufactured below 400 MPa compression pressure, and lactose tablets manufactured below 50 MPa compression pressure with a modified Heckel approach due to an inaccurate computation of  $\rho_{particle}$  (Table 1). The YPpl and YPel (compacted below 200 MPa) of starch calculated with the new approach were 1.57–3.06, and 1.97–3.65 times greater than those calculated with a general approach, respectively. A general and new approach YPpl and YPel of starch compacted below 400 MPa were significantly different ( $0.000006 \leq p \leq 0.00160$ ). The YPpl starch calculated (compacted above 400 MPa) with a new and modified Heckel approach were 1.81–3.06 times greater than general approach starch YPpl. Starch YPpl values calculated with different approaches were

significantly different ( $0.000008 \leq p \leq 0.00006$ ). The YPel starch (compacted below 400 MPa) calculated with a general and new approach were also significantly different ( $0.000006 \leq p \leq 0.00082$ ).

#### 4.2.3. Validation of new approach with modified Heckel approach

The differences between the YPpl and YPel values of MCC and lactose tablets (compressed above 100 MPa compression pressure) calculated with a new and modified Heckel approach were statistically insignificant ( $0.07 \leq p \leq 0.99$ ). It confirms that the Heckel parametrization performed with  $\rho_{PP}$  and  $\rho_{particle}$  could provide similar results. It is important to note that the new approach was able to compute Heckel parameters for poorly compacting materials like starch in the studied compression pressure ranges. This was not possible with a modified Heckel approach. The YPpl and YPel values of starch compacted above 400 MPa calculated with a new and modified Heckel approach were significantly different ( $0.00001 \leq p \leq 0.0023$ ).

A new approach of Heckel parameterization distinctly demonstrated its ability to handle negative porosity issues regardless of their deformation properties, compaction properties, and applied compression pressure. These capabilities were not observed with the general and modified Heckel approach.

## 5. Conclusions

A general approach of Heckel analysis utilizes  $\rho_{P0}$ . It leads to a negative porosity issue in the high-pressure range due to an increase in  $\rho_{BP}$  than  $\rho_{P0}$ . A new approach of using  $\rho_{PP}$  for ‘in-die’ Heckel parametrization demonstrated its immunity for negative porosity issues. The  $\rho_{PP}$  is always higher than  $\rho_{P0}$ . Thus,  $\rho_{PP}$  seems greater than  $\rho_{BP}$  during ‘in-die’ parametrization, specifically in the high-pressure region of the compression cycle. This keeps ‘in-die’ Heckel parametrization in Zone-I

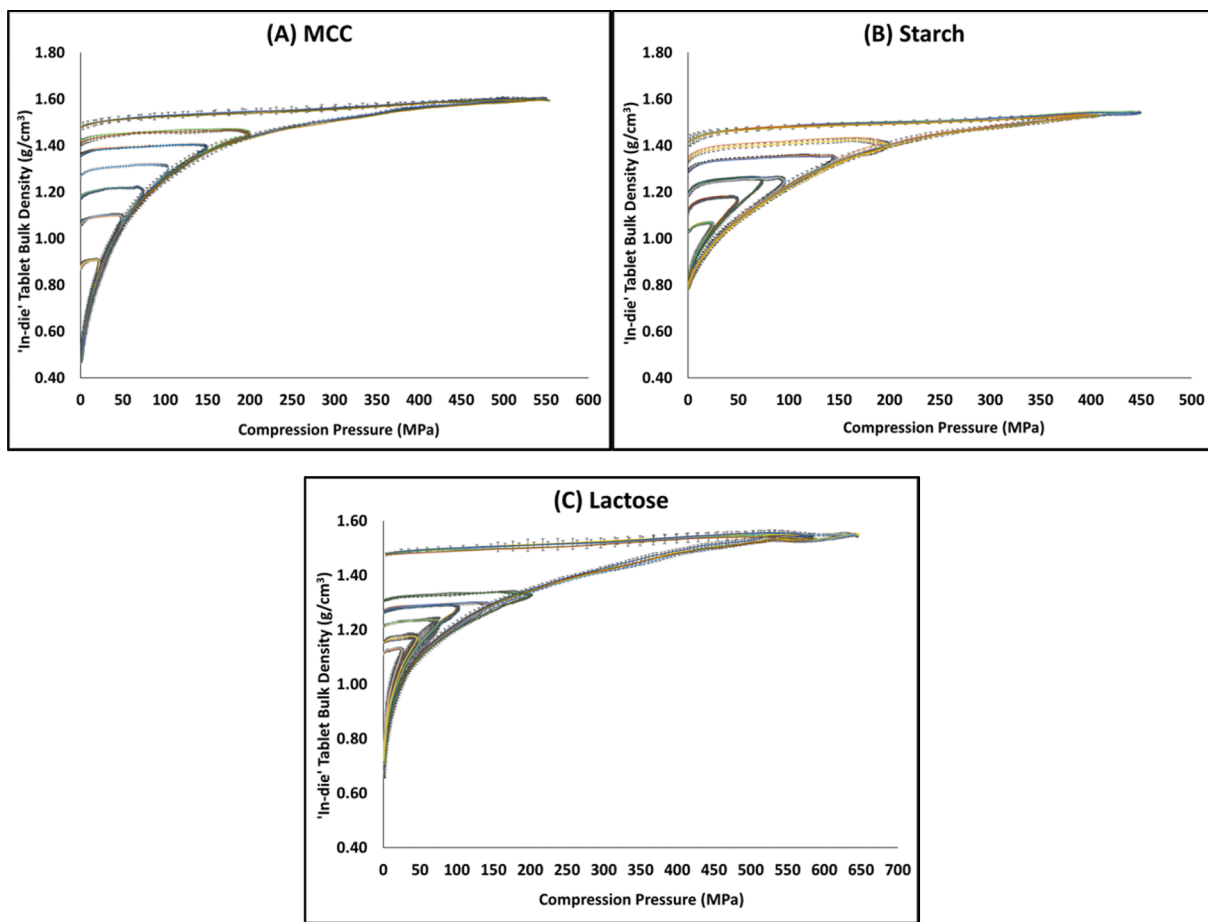


Fig. 6. 'In-die' tablet bulk density (g/cm<sup>3</sup>) vs. compression pressure (MPa) plots obtained for (A) MCC; (B) Starch; and (C) Lactose at applied compression pressure (three replicate strokes for each applied compression pressure plotted with standard deviation).

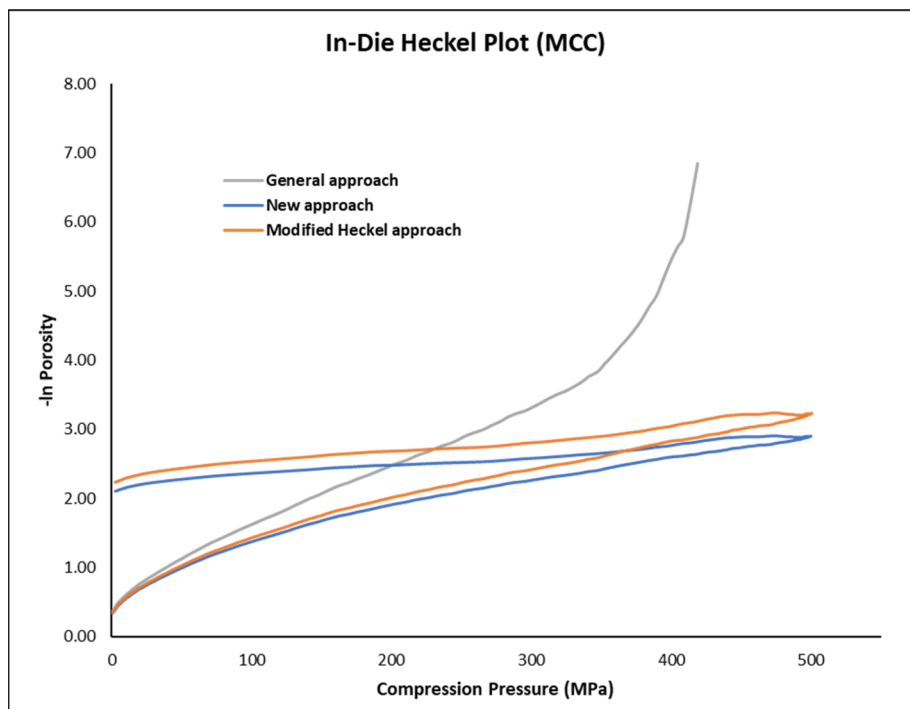


Fig. 7. An 'in-die' Heckel plot of individual MCC tablet compressed at compression pressure of 500.2 MPa with a general approach ( $\rho_{p0} = 1.57 \text{ g/cm}^3$ ), new approach ( $\rho_{pp} = 1.68 \text{ g/cm}^3$ ), and modified Heckel approach ( $\rho_{particle} = 1.65 \text{ g/cm}^3$ ).

( $V_B > V_P$ ), which is devoid of a negative porosity issue. Therefore, the present work demonstrated that the application of  $\rho_{PP}$  in the Heckel relative density calculations allows for an efficient use of the compression and decompression phase without having negative porosity issues. The new approach was validated with the modified Heckel approach.

A proposed new approach has demonstrated its ability to utilize the full potential of dynamic compression profiles generated with a limited amount of material regardless of materials intrinsic deformation properties or applied compression pressure. The full Heckel plot devoid of a negative porosity offers yield pressure values reflecting material deformation and tablet elastic recovery from the compression and decompression phase, respectively. This is very important specifically in an early development stage. Such information provides valuable insights into the intrinsic material compaction performance necessary to build a scientifically sound prototype formulations for further product developments.

#### CRedit authorship contribution statement

**Devang Patel:** Conceptualization, Methodology, Investigation, Writing – original draft. **Vivek D. Patel:** Conceptualization, Methodology, Investigation, Writing – original draft. **Robert Sedlock:** Supervision, Project administration. **Rahul V. Haware:** Conceptualization, Investigation, Writing – review & editing, Supervision.

#### Declaration of Competing Interest

The authors declare that they have no known competing financial interests or personal relationships that could have appeared to influence the work reported in this paper.

#### Acknowledgments

The authors are thankful to John C. Sturgis at Natoli Scientific - A Division of Natoli Engineering Company, Inc. for calibration of the Presster™.

#### Appendix A. Supplementary data

Supplementary data to this article can be found online at <https://doi.org/10.1016/j.ijpharm.2022.122205>.

#### References

- Bassam, F., York, P., Rowe, R.C., Roberts, R.J., 1990. Young's modulus of powders used as pharmaceutical excipients. *Int. J. Pharm.* 64, 55–60. [https://doi.org/10.1016/0378-5173\(90\)90178-7](https://doi.org/10.1016/0378-5173(90)90178-7).
- Cartensen, J.T., Geoffroy, J.M., Dellamonica, C., 1990. Compression characteristics of binary mixtures. *Powder Technol.* 62, 119–124. [https://doi.org/10.1016/0032-5910\(90\)80074-9](https://doi.org/10.1016/0032-5910(90)80074-9).
- Çelik, M., 2011. Pharmaceutical powder compaction technology, Second, ed. Pharmaceutical Powder Compaction Technology. Informa Healthcare, New York. <https://doi.org/10.3109/9781420089189>.
- Çelik, M., 1992. Overview of compaction data analysis techniques. *Drug Dev. Ind. Pharm.* 18, 767–810. <https://doi.org/10.3109/03639049209058560>.

- Çelik, M., Okutgen, E., 1993. A feasibility study for the development of a prospective compaction functionality test and the establishment of a compaction data bank. *Drug Dev. Ind. Pharm.* 19, 2309–2334. <https://doi.org/10.3109/03639049309047193>.
- Denny, P.J., 2002. Compaction equations: A comparison of the Heckel and Kawakita equations. *Powder Technol.* 127, 162–172. [https://doi.org/10.1016/S0032-5910\(02\)00111-0](https://doi.org/10.1016/S0032-5910(02)00111-0).
- Fell, J.T., Newton, J.M., 1971. Effect of particle size and speed of compaction on density changes in tablets of crystalline and spray-dried lactose. *J. Pharm. Sci.* 60, 1866–1869. <https://doi.org/10.1002/jps.2600601223>.
- Fichtner, F., Rasmuson, Å.C., Alander, E.M., Alderborn, G., 2007. Effect of preparation method on compactability of paracetamol granules and agglomerates. *Int. J. Pharm.* 336, 148–158. <https://doi.org/10.1016/j.ijpharm.2006.11.046>.
- Govedarica, B., Ilić, I., Sibanc, R., Dreu, R., Srčić, S., 2012. The use of single particle mechanical properties for predicting the compressibility of pharmaceutical materials. *Powder Technol.* 225, 43–51. <https://doi.org/10.1016/j.powtec.2012.03.030>.
- Haware, R.V., Bauer-Brandl, A., Tho, I., 2010a. Comparative evaluation of the powder and compression properties of various grades and brands of microcrystalline cellulose by multivariate methods. *Pharm. Dev. Technol.* 15, 394–404. <https://doi.org/10.3109/10837450903262041>.
- Haware, R.V., Tho, I., Bauer-Brandl, A., 2010b. Evaluation of a rapid approximation method for the elastic recovery of tablets. *Powder Technol.* 202, 71–77. <https://doi.org/10.1016/j.powtec.2010.04.012>.
- Haware, R.V., Tho, I., Bauer-Brandl, A., 2009a. Application of multivariate methods to compression behavior evaluation of directly compressible materials. *Eur. J. Pharm. Biopharm.* 72, 148–155. <https://doi.org/10.1016/j.ejpb.2008.11.008>.
- Haware, R.V., Tho, I., Bauer-Brandl, A., 2009b. Multivariate analysis of relationships between material properties, process parameters and tablet tensile strength for  $\alpha$ -lactose monohydrates. *Eur. J. Pharm. Biopharm.* 73, 424–431. <https://doi.org/10.1016/j.ejpb.2009.08.005>.
- He, Y., Evans, T.J., Shen, Y.S., Yu, A.B., Yang, R.Y., 2018. Discrete modelling of the compaction of non-spherical particles using a multi-sphere approach. *Miner. Eng.* 117, 108–116. <https://doi.org/10.1016/j.mineng.2017.12.013>.
- Heckel, R.W., 1961a. Density-pressure relationships in powder compaction. *Trans. Metall. Soc. AIME* 221, 671–675.
- Heckel, R.W., 1961b. An Analysis of Powder Compaction Phenomena. *Trans. Metall. Soc. AIME* 221, 1001–1008.
- Kawakita, K., 1963. Compression of powders. *J. Japan Soc. Powder Powder Metall.* 10, 236–246. <https://doi.org/10.2497/jjspm.10.236>.
- Kuentz, M., Leuenberger, H., 1999. Pressure susceptibility of polymer tablets as a critical property: A modified Heckel equation. *J. Pharm. Sci.* 88, 174–179. <https://doi.org/10.1021/js980369a>.
- Micromeritics, 2019. AccuPyc II 1345 gas displacement pycnometry system - Operator manual. Micromeritics Instrument Corp, USA.
- Newton, J.M., Rowley, G., Fell, J.T., Peacock, D.G., Ridgway, K., 1971. Computer analysis of the relation between tablet strength and compaction pressure. *J. Pharm. Pharmacol.* 23, 195S–201S. <https://doi.org/10.1111/j.2042-7158.1971.tb08789.x>.
- Paronen, P., 1986. Heckel plots as indicators of elastic properties of pharmaceuticals. *Drug Dev. Ind. Pharm.* 12, 1903–1912. <https://doi.org/10.3109/03639048609042616>.
- Roberts, R.J., Rowe, R.C., 1987. The Young's modulus of pharmaceutical materials. *Int. J. Pharm.* 37, 15–18. [https://doi.org/10.1016/0378-5173\(87\)90004-4](https://doi.org/10.1016/0378-5173(87)90004-4).
- Rue, P.J., Rees, J.E., 1978. Limitations of the Heckel relation for predicting powder compaction mechanisms. *J. Pharm. Pharmacol.* 30, 642–643. <https://doi.org/10.1111/j.2042-7158.1978.tb13347.x>.
- Shapiro, I., Kolthoff, I.M., 1947. Studies on the aging of precipitates and coprecipitation. XXXVIII: The compressibility of silver bromide powders. *J. Phys. Colloid Chem.* 51, 483–493. <https://doi.org/10.1021/j150452a015>.
- Sonnergaard, J.M., 1999. A critical evaluation of the Heckel equation. *Int. J. Pharm.* 193, 63–71. [https://doi.org/10.1016/S0378-5173\(99\)00319-1](https://doi.org/10.1016/S0378-5173(99)00319-1).
- Sun, C., 2004. A novel method for deriving true density of pharmaceutical solids including hydrates and water-containing powders. *J. Pharm. Sci.* 93, 646–653. <https://doi.org/10.1002/jps.10595>.
- van den Ban, S., Goodwin, D.J., 2017. The Impact of Granule Density on Tableting and Pharmaceutical Product Performance. *Pharm. Res.* 34, 1002–1011. <https://doi.org/10.1007/s11095-017-2115-5>.
- Walker, E.E., 1923. The properties of powders. Part VI. The compressibility of powders. *Trans. Faraday Soc.* 19, 73–82. <https://doi.org/10.1039/tf9231900073>.
- Yu, A.B., Hall, J.S., 1994. Packing of fine powders subjected to tapping. *Powder Technol.* 78, 247–256. [https://doi.org/10.1016/0032-5910\(93\)02790-H](https://doi.org/10.1016/0032-5910(93)02790-H).